Published in final edited form as:
Neuroscience. 2009 March 17; 159(2): 647–656. doi:10.1016/j.neuroscience.2008.12.053.

Dynein motor contributes to stress granule dynamics in primary neurons

Nien-Pei Tsai, **Yao-Chen Tsui**, and **Li-Na Wei**
Department of Pharmacology, University of Minnesota Medical School, Minneapolis, MN 55455, USA

Abstract

Mobilization and translation of mRNAs, two important events believed to involve stress granules (SGs), in neurons are important for their survival and activities. However, the formation and disassembly of SGs in neurons remains unclear. By using an arsenite-induced neuronal stress model of primary spinal cord neuron cultures, we demonstrate the formation of SGs that contain common SG components and RNAs in both stressed neuronal cell bodies and their neurites. By employing siRNA knockdown, we discovered that dynein motor subunit localizes in SG, and is important for SG assembly in neurons. Under stress, dynein motor subunit also facilitates translational repression and enhances the formation and integrity of SG in neurons. By blocking the energy source of dynein motor, both the formation and disassembly of SG are attenuated. These findings demonstrate, for the first time, that dynein motor complex plays a critical role in the dynamics of neuronal SGs, as well as translation of certain mRNAs.

Keywords

mRNA; translation; primary neurons; stress granules; dynein; neurites

Introduction

Cells assemble stress granules (SGs), as a protective mechanism, in response to various stressful conditions such as upon exposure to environmental toxins like arsenite or a high temperature, or as a result of translational inhibition (Anderson and Kedersha, 2006, Kiebler and Bassell, 2006). Although this important phenomenon has been observed in most cell types (Kim et al., 2006, Vessey et al., 2006), the dynamics of SG are still poorly understood.

SG assembly can be initiated by auto-aggregation of the prion-like C-termini of T cell internal antigen-1 (TIA-1) that promotes polysome disassembly, rendering mRNA mobilization into SGs (Gilks et al., 2004). Multiple RNA-binding proteins lacking prion-like domains are also recruited to SGs (Guil et al., 2006, Stohr et al., 2006, Baguet et al., 2007, Gallois-Montbrun et al., 2007), suggesting the involvement of some sorts of active transport machinery in the formation of SGs. In this study, we ask several specific questions: a) how these SGs are assembled and b) whether it is mediated by any transport machinery.

*Correspondence: Li-Na Wei, Department of Pharmacology, University of Minnesota Medical School, 6-120 Jackson Hall, 321 Church St. SE, Minneapolis, MN 55455, USA. Tel (612) 6259402, Fax (612) 6258408, email weixx009@umn.edu.

In order to address these questions specifically in neurons, we employed primary spinal cord neuron cultures stressed by arsenite treatment and demonstrated that SGs could be formed in both the soma and neurites of primary neurons upon arsenite stress, to which cellular RNAs were recruited. P19 embryonal carcinoma cells were used for biochemical studies, which demonstrated a role for dynein in facilitating SG integrity and translational repression in cells under stress. This study not only demonstrates SG formation in primary neurons including their soma and neurites, but also uncovers the specific motor apparatus involved in this process.

Experimental Procedures

All the experiments involving animals in this study have been approved by the University's Institutional Animal Care and Use Committee, and conform to the regulatory standard. The number of animals and the animal suffering were minimized throughout this study.

Antibodies and Reagents

Antibodies were from Santa Cruz Biotechnology (Santa Cruz, CA) (anti-TIA-1, anti-DLC2A, anti-eIF2α, anti-phospho-eIF2α and anti-HuR), Sigma-Aldrich (St. Louis, MO) (anti-Actin), and Genetex (San Antonio, TX) (anti-Staufen 1). Sodium Arsenite and EHNA were from Sigma-Aldrich (St. Louis, MO). AMP-PNP was from Roche Applied Science (Indianapolis, IN). HiLyte Fluor 647 conjugated Streptavidin was from AnaSpec (San Jose, CA). Biotinylated Oligo(dT) was from Promega (Madison, WI). Dynein light chain 2A siRNAs were from Qiagen (Valencia, CA). (HP genome wild series). ^{35}S-Methionine/Cysteine was from MP Biomedicals (Irvine CA).

Plasmid construction

Flag-tagged DLC2A was made by inserting the full-length DLC2A cDNA amplified with a primer pair (5′- GGA TCC GCA GAT GTG GAG GAA ACA CTC-3′ and 5′- GCT AGC TTA TTC AGT TGG ATT CTG GAT C -3′) into BglII/NheI sites of a Flag-tag expression vector pCMX (Umesono et al., 1991).

Spinal cord neuron culture and fluorescence in situ hybridization

Primary spinal cord neuron culture was described previously (Tsai et al., 2006). In brief, primary neurons were dissected from 2 to 5 days newborn rats and dissociated into single neurons by treating with 50 units of collagenase for 30 min and 0.05% trypsin-EDTA for 5 min consequently. Suspended neurons were plated on 0.1 mg/ml poly-D-lysine-coated 24-well plates. Neurons were maintained in a medium containing MEM with 10% FBS, 1% N2, and 1% penicillin/streptomycin for 3 days, and subjected to arsenite treatment, followed by immunohistochemistry or fluorescence in situ hybridization. Fluorescence in situ hybridization was performed as described (Bassell et al., 1998) with some modifications. In brief, spinal cord neuron cultures were grown in 24-well plates. On the day of experiment, cultures were washed with 1X PBS and fixed for 10 minutes at room temperature with 4% formaldehyde in 1X PBS. To enhance the reaction in cytoplasm, fixation was conducted at this moment with no further permeabilization (such as treatment by 10% acetic acid). After washing with 1X PBS for three times, cells were rehydrated for 5 minutes in 2X SSC (300 mM NaCl and 30 mM sodium citrate, pH 7.0) and 50% formamide. Cells were then hybridized with 5 ng biotinylated oligo (dT) in 15% formamide at 37°C for 4 hours. After washing with 1X PBS for three times, HiLyte Fluor 647-conjugated Streptavidin was diluted (1:1000) and applied onto fixed cells for 1 hour. After washing and staining with DAPI for 5 minutes, cells were examined under an inverted fluorescence microscope and images were acquired and exported with Adobe Photoshop 7.0 software for color and imaging merging.

Stress induction and immunohistochemistry

Stress was induced by adding 0.5 mM sodium arsenite for different time periods according to experimental designs. Cells were then fixed with -20°C stored methanol for 15 minutes. After blocking with 5% calf serum for 30 minutes, primary antibodies were 1:200 diluted with 5% calf serum and applied onto fixed cells for at least 4 hours. After three times PBS washing, 1:500 diluted Cy3, FITC or AMCA-conjugated secondary antibodies were applied onto cells for another 2 hours in dark. With additional washing for three times and 5-minute DAPI staining, cells were observed with inverted fluorescence microscope.

^{35}S-Methionine/Cysteine incorporation

^{35}S-Met/Cys incorporation for total translational rate and for translation of target proteins were performed by adding 0.05 mCi ^{35}S-Met/Cys onto 5 cm and 75% confluent plates for labeling. To determine the total translational rate using metabolic labeling, at different time points cells were harvested, washed with 1X PBS and lysed by sonication. 100 μg total protein was quantified for ^{35}S incorporation with a liquid scintillation counter. To determine the translation of KOR, Actin and HSP70, 500 μg total protein from each time point was used in specific immunoprecipitation. Precipitated proteins were resolved on an 8% SDS-PAGE which was dried and exposed to a PhosphorImager (Molecular Dynamics, Sunnyvale, CA). Quantification was conducted using the ImageJ software.

Western blotting, immunoprecipitation and siRNA experiments

Western blotting and immunoprecipitation were as previously described (Tsai et al., 2007) with slight modification. In brief, to enhance immunopurification of less soluble proteins in SG, cell lysates were extensively sonicated for 20 seconds in a buffer (0.5% SDS, 1% Triton X-100, 1 mM EDTA, 1M NaCl, 20 mM Tris-HCl, pH 8.0) and incubated with the specific antibody overnight at 4°C with continuous shaking. Protein G beads (Billerica, Massachusetts) (Millipore) were then added for another one hour followed by washing for three time with PBS and SDS-PAGE and western blotting analyses. siRNAs from Qiagen were prepared as manufacturer suggested and transfetced with HyperFect transfection reagent (Valencia, CA) (Qiagen). Two independent sequences of DLC2A (1st target sequence: CCC AAG AAT AAT AGT GCT AAT; 2nd target sequence: CTG TGT CAT TCC TTA ATT TAA) were applied and all experiments were repeated at least three times.

Protease resistance assay

Assay was performed as described previously (Gilks et al., 2004). In brief, cytoplasmic protein was prepared by NE-PER Nuclear and Cytoplasmic Extraction Reagents from Pierce (Rockford, IL). 100 μg total cytoplasmic protein was digested with Protease K for 4 minutes at 37°C. Samples were quickly added with sample buffer and subjected to SDS-PAGE and Western blotting analyses. The experiments were repeated three times and the intensities of TIA-1 obtained from Western blots were quantified with the ImageJ software.

Cell counting and Statistical analysis

In each experiment, 100 cells were scored to determine the percentage of cells with SGs (defined as approximately 1 μm in the diameter, or larger, distinct granules observed in images merged with FITC and Cy3 signals) for both primary neurons and P19 cells. Three experiments were conducted to obtain statistical results, presented as means ± standard deviations and analyzed with Student's *t*-test where $P < 0.05$ was considered as significant.

Results

Arsenite induced formation of SGs in primary spinal cord neurons

To validate SG formation in primary neurons, we applied 0.5 mM sodium arsenite in primary spinal cord neuron cultures for 20 minutes. In the control culture, immunoreactivities of both TIA-1 and another SG component, Hu antigen R (HuR) (Kedersha and Anderson, 2002), appeared strong in nucleus, and relatively weak but homogenous in both the cytoplasm and neurites (Fig. 1A top, and Fig. 1B left). In the arsenite-stressed cultures (Fig. 1A bottom and Fig. 1B right), distinct overlapping punctate granules, mostly larger than 1 μm (Ivanov et al., 2003), of TIA-1 and HuR appeared in both the cytoplasm and neurites. Since it was suggested that phosphorylation of eIF2α initiated SGs formation (Kedersha et al., 2002), the status of phospho-eIF2α in stressed neurons was monitored with a specific anti-phospho-eIF2α antibody (Fig. 1C). We indeed found enhanced phosphorylation of eIF2α in these neurons stressed with arsenite and justified our stress conditions. All together, the results suggest that SG formation in these primary neurons, including their neurites, is likely to be a common process. However, some partially overlapping or non-overlapping puncta were also observed, suggesting that not all the SGs contained the same evenly distributed components, which was also observed previously in other types of cells (Nonhoff et al., 2007). Furthermore, some very small granules were occasionally seen in unstressed cells, as also observed in other neuronal systems and suggested to represent certain RNP complexes (Barbee et al., 2006, Ferrari et al., 2007). Finally, to confirm these punctate granules were true SGs, we applied cycloheximide, a drug known to block SG formation (Vessey et al., 2006), in arsenite stress experiments. As shown in Fig 1A bottom and Fig 1B right, TIA-1 aggregates were effectively inhibited by cycloheximide, confirming the punctate granules detected in this system as legitimate SGs. Together these results unambiguously demonstrate the formation of SGs in both the soma and the extended neurites of stressed primary neurons.

Studies of other experimental systems indicated that SGs, in addition to playing a role in translational repression, were the triage centers of RNAs during stress. We thus performed experiments to determine whether RNAs could be recruited to the SGs in stressed neurons, including their neurites. In order to address this question in a non-biased manner with respect to the physiological representation of total cellular mRNA pool, we performed fluorescence *in situ* hybridization with biotinylated Oligo(dT) on the normal and stressed cultures. This was conducted without breaking down nuclear membrane in order to enrich probes in the cytoplasm (see Experimental Procedures). It appeared that the otherwise evenly distributed mRNA (stained with fluorescence-conjugated streptavidin) in the control culture (Fig. 1D top left and top right) became concentrated in the TIA-1-positive granules in both the cytoplasm and neurites of the stressed neurons (Fig. 1D left bottom and right bottom). Statistical analyses showed that 73% of stressed cells were SG-positive, indicated by punctate Oligo(dT) granules, as compared to a merely 5% of the control cells that were SG-positive. These experiments validate that the vast majority of the endogenous mRNA pool is indeed enriched in the SGs of stressed neurons.

Dynein motor subunits are located and required for SG formation

It was indicated that the aggregation of TIA-1 initiated the formation, or enhanced the integrity, of SGs. However, it was unclear how the other SG components were mobilized to SGs and if the process was mediated by any active transport mechanism. We then speculated a role for the known RNA transport machinery such as dynein (Ling et al., 2004, Lee et al., 2006) in SG formation, and therefore examined if dynein could be co-localized with SGs (Fig. 2A and 2B). The results showed that in arsenite-stressed culture, TIA-1 became co-localized with dynein light chain 2A (DLC2A), one of the critical subunit in dynein complex (Lo et al., 2007, Wanschers et al., 2008), in punctate granules (Fig 2A right), which was also apparent in the

extended neurite areas (Fig 2B right). These results reveal that dynein motors move into the close proximity of SGs in both soma and neurites of stressed neurons. To further validate this observation using biochemical assays, which required a significant amount of material, we employed a mouse embryonal carcinoma cell line P19 that has been successfully used in our previous studies of RNA mobilization and localized translational control of neuronal proteins (Bi et al., 2003, Tsai et al., 2006). We first confirmed that DLC2A was also co-localized with the SG marker protein, TIA-1, in arsenite-treated P19 cells (Fig 2C). As shown in Fig 2D, formation of the dynein motor/SG components (DLC2A/HuR/TIA-1 complex) in arsenite-stressed P19 cultures (for 30 or 60 minutes) was also increased. It was also noticed that the DLC2A signals in the nucleus of both primary neurons and P19 cells were also altered, which suggests that arsenite treatment might have caused some rearrangement of the motor complex in the nucleus; but the mechanism remains to be determined.

To assess if the DLC2A is required for SG formation, we applied two independent siRNAs of DLC2A to knockdown endogenous DLC2A in primary neurons (Fig 3A shows one set of data). The results showed that silencing DLC2A abolished SG formation in stressed neurons (as low as 26% SG-positive cells in the DLC2A-silenced culture, compared to 78% SG-positive cells in the control culture, $P < 0.05$). Similar phenomenon was also observed in P19 cells shown in Fig 3B. The results demonstrated that silencing DLC2A abolished SG formation in stressed cells (to as low as 32% SG-positive in the DLC2A-silenced culture, compared to 85% SG-positive in the control culture, $P < 0.05$). Importantly, with biochemical method, silencing DLC2A with siRNA (Fig. 3C) reduced co-precipitated complexes containing SG components in response to arsenite stress, as indicated by the loss in the co-precipitated complexes containing common SG components including TIA-1, HuR and Staufen 1 (Stau1) (Thomas et al., 2005). These results suggest a general role for dynein motor activity in SG formation in different cell types including primary neurons and P19, and justify P19 as a valid experimental system for subsequent mechanistic studies.

Dynein motor subunit enhances the integrity of TIA-1 complexes

It was proposed that SG integrity was regulated by TIA-1 aggregates (Gilks et al., 2004). We then tested if dynein affected SG integrity, which could be assessed by protease sensitivity of TIA-1 complexes. As shown in Fig 4A, TIA-1 complexes in normal stressed cells were sensitive to protease treatment at the concentration of 0.8-1.6 μg/ml, but those in DLC2A transfected (by transient transfection with Flag-DLC2A), stressed cells became more resistant to protease (sensitive to concentrations higher than 1.6 μg/ml). Transfection efficiency was monitored with the anti-Flag antibody (bottom middle of Fig 4A). On the contrary, in DLC2A-silenced, stressed cells, TIA-1 complexes were more sensitive to protease (sensitivity lowered to the concentration range of 0.4-0.8 μg/ml). The intensities of TIA-1 signals were quantified from three-independent experiments and shown in Fig 4B. The data demonstrate that dynein motors can slightly enhance the integrity of TIA-1 complexes, or the aggregation of sub-SG components, thereby facilitating SG formation in stressed cells.

To determine if altering the level of dynein alone could affect SG formation rate, we transiently transfected P19 cells with Flag-DLC2A or DLC2A siRNA, and examined SG formation under arsenite stress. By scoring SG-positive, Flag-DLC2A transfected or untransfected cells, we detected enhancement in SG formation elicited by exogenous DLC2A during the initial phase of stress (first 15- or 30-minute arsenite treatment). However, silencing DLC2A reduced the number of SG-positive cells (Fig 4C).

To further examine whether dynein could also enhance translational repression by stress, an accepted role for SGs, we conducted metabolic labeling experiments to determine the total translational rates as shown in Fig 5A. As compared to the control stressed cells, increased ^{35}S-Methionine/Cysteine incorporation was detected in the DLC2A-silenced and

stressed cells at the time points of 40- and 50-minute labeling, whereas decreased ^{35}S-Methionine/Cysteine incorporation was detected in the Flag-DLC2A transfected and stressed cells at these time points. The difference was slight but statistically significant. To validate this result, we used the translation of known SG-exclusive transcript such as heat shock protein 70 (HSP70) (Kedersha and Anderson, 2002) as a control, and monitored *de novo* protein synthesis of two SG-recruited transcripts, kappa opioid receptor (KOR) and actin mRNAs (Tsai et al., 2008). The result consistently showed that, under arsenite treatment, translation of these two transcripts, especially the kappa opioid receptor transcript, was enhanced in DLC2A-silenced cells and reduced in Flag-DLC2A transfected cells (Fig 5B) as compared to control cells. Therefore we conclude that, in stressed cells, the dynein motor facilitates SG formation and translational repression.

Dynein motor subunit is critical for both SG formation and disassembly

To verify if SG formation required the specific motor's activity, we tested the effects of two motor inhibitors that could block energy consumption by motor complexes (Fig 6A and 6B). One is dynein motor inhibitor Erythro-9-[3-(2-hydroxynonyl)] adenine (EHNA) and the other is a commonly used kinesin motor inhibitor adenosine 5′-(β,γ-imido) triphosphate (AMP-PNP) (Ravikumar et al., 2005). Clearly, the formation of SGs in arsenite-stressed primary spinal cord neurons (Fig 6A) and P19 cells (Fig 6B) was blocked by EHNA, but not by AMP-PNP. Quantitative analyses revealed 25% SG-positive spinal cord neurons and 20% SG-positive P19 cells in the EHNA-treated cultures as compared to 69% SG-positive spinal cord neurons and 66% SG-positive P19 cells in the AMP-PNP-treated cultures and 73% SG-positive spinal cord neurons and 71% SG-positive P19 cells in the cultures without these drugs. There was a slight reduction in the percentage of SG-positive cells following AMP-PNP treatment, suggesting that this drug might have disturbed energy homeostasis that slightly affected SG formation, but the effect was not as significant as that caused by EHNA ($P < 0.05$). These results consistently demonstrate that dynein motors, as well as the activities, are required for SG formation. By applying immunoprecipitation with anti-TIA-1 antibody to precipitate known associated SG components, such as HuR and Staufen 1, from stressed P19 cells treated with EHNA or AMP-PNP, a very similar result was obtained as shown in Fig 6C. As the dose of EHNA, but not AMP-PNP, was raised, the amount of co-precipitated complex was gradually decreased (1st and 3rd panels from top). These results consistently demonstrated that Dynein motor, as well as its activity, was required for SG formation.

To determine if motor complexes were also required for efficient SG disassembly, we applied EHNA, or AMP-PNP, to P19 cultures following arsenite stress and then allowed to recover in fresh medium. We monitored the retaining of SGs by staining cultures with anti-TIA-1 at different time points of recovery (Fig 7A). It appeared that EHNA, but not AMP-PNP, also delayed SG disassembly during the recovery phase. This was more evident after 20 or 40 minutes of recovery where more apparent SGs were retained in the EHNA-treated cultures. Quantification data confirmed a more significant effect of EHNA in later time points of recovery (Fig 7B). It was noticed that the sizes of SGs in EHNA-treated cells at 20- and 40-minute recoveries were smaller than the SGs detected in the initial time point. This suggests that, in EHNA-treated cells, disruption of SG can be delayed; therefore the intermediate forms (transition between SGs and RNP complexes) are seen. All together, these results suggest, for the first time, that it is also dynein, but not kinesin, motor complexes that are involved in efficient SG disassembly during post-stress recovery.

Discussion

In summary, by using an arsenite-induced stress model of primary spinal cord neurons, we have demonstrated the formation of SGs not only in the soma but also in the neurites of these

primary neurons. Further, this requires, or is mediated by, the active transport machinery that utilizes the dynein motor complex. However, based on the observation of very small granules in cells treated with a high concentration of EHNA (indicated by arrow heads in Fig 6A and 6B) and the elevated phosphorylation of eIF2α observed in EHNA-treated or DLC2A-silenced cells after arsenite treatment (Supplemental Fig 1), it is likely that local aggregation is initiated prior to more significant granule mobilization, elicited by dynein motors, to form obvious SGs. It is therefore suggested that dynein motors play a major role in coordinating the aggregation of sub-granules into larger granules seen as SGs in cells under stress, which is critical for translational repression and the integrity of SGs. Given that dynein was absent from polysomes and could not directly interact with mRNA species (data not shown), dynein is more likely to play a role, primarily, in coordinating or mobilizing protein complexes, rather than to directly recruit mRNAs.

With the detection of SGs in neurites, it is tempting to speculate that localized RNA-based regulatory events, such as RNA mobilization and translational regulation coordinated by SGs in stressed cells also play roles in protecting neurites during stress. It is known that local translation in the neurites can regulate multiple neuronal activities (Wu et al., 2005, Leung et al., 2006). Under unfavorable conditions, cells respond by first halting their global translation system while allowing translation of specific components that are crucial for their survival such as heat shock proteins (Kedersha and Anderson, 2002). Our results suggest that neurites also employ this type of protecting mechanism, locally, which may be far more effective and efficient than waiting for a global response from the soma. Recently, we have demonstrated mobilization of mRNA of the kappa opioid receptor from soma to axons of DRG neurons, where it could be stimulated for local translation in axons (Bi et al., 2006). To this end, it is potentially interesting to examine whether SGs, or their components, could be related to either the transport or translation of specific mRNA species. It has been reported that local translation in neuronal cells is regulated by specialized RNA granules containing Staufen protein (Krichevsky and Kosik, 2001). It will be important to determine if these RNA granules and SGs are structurally or functionally related in the neuritis and to understand the relationship between local translation and neuronal activities, such as synaptic plasticity and neuron degeneration.

We have previously shown that disassembly of SGs could be facilitated by the activation of FAK-Grb7 signaling pathway (Tsai et al., 2008). However, it was puzzling if SG components were actively distributed, or mobilized, presumably back to their normal location, or they were randomly diffused, when stress was terminated. This current report demonstrates, for the first time, that dynein motor is also involved in the disassembly of SGs during post-stress recovery. These results suggest that the active transport machinery plays an important role in sorting SG components both during stress and post-stress recovery. The physical association of dynein motor complex with SG components also explains the efficient disassembly of SGs during the recovery phase. Whether and how the cells differentiate the activity of dynein motor during the formation and disassembly of SGs, and if there are specific “cargos” to transport SG components, are important issues to be addressed in the future.

Supplementary Material

Refer to Web version on PubMed Central for supplementary material.

Acknowledgements

This work is supported in part by NIH Grants DA11190, DA11806, DK54733, DK60521 and K02-DA13926 to LNW.

References

Anderson P, Kedersha N. RNA granules. J Cell Biol 2006;172:803–808. [PubMed: 16520386]

Baguet A, Degot S, Cougot N, Bertrand E, Chenard MP, Wendling C, Kessler P, Le Hir H, Rio MC, Tomasetto C. The exon-junction-complex-component metastatic lymph node 51 functions in stress-granule assembly. J Cell Sci 2007;120:2774–2784. [PubMed: 17652158]

Barbee SA, Estes PS, Cziko AM, Hillebrand J, Luedeman RA, Coller JM, Johnson N, Howlett IC, Geng C, Ueda R, Brand AH, Newbury SF, Wilhelm JE, Levine RB, Nakamura A, Parker R, Ramaswami M. Staufen- and FMRP-containing neuronal RNPs are structurally and functionally related to somatic P bodies. Neuron 2006;52:997–1009. [PubMed: 17178403]

Bassell GJ, Zhang H, Byrd AL, Femino AM, Singer RH, Taneja KL, Lifshitz LM, Herman IM, Kosik KS. Sorting of beta-actin mRNA and protein to neurites and growth cones in culture. J Neurosci 1998;18:251–265. [PubMed: 9412505]

Bi J, Hu X, Loh HH, Wei LN. Mouse kappa-opioid receptor mRNA differential transport in neurons. Mol Pharmacol 2003;64:594–599. [PubMed: 12920195]

Bi J, Tsai NP, Lin YP, Loh HH, Wei LN. Axonal mRNA transport and localized translational regulation of kappa-opioid receptor in primary neurons of dorsal root ganglia. Proc Natl Acad Sci U S A 2006;103:19919–19924. [PubMed: 17167054]

Ferrari F, Mercaldo V, Piccoli G, Sala C, Cannata S, Achsel T, Bagni C. The fragile X mental retardation protein-RNP granules show an mGluR-dependent localization in the post-synaptic spines. Mol Cell Neurosci 2007;34:343–354. [PubMed: 17254795]

Gallois-Montbrun S, Kramer B, Swanson CM, Byers H, Lynham S, Ward M, Malim MH. Antiviral protein APOBEC3G localizes to ribonucleoprotein complexes found in P bodies and stress granules. J Virol 2007;81:2165–2178. [PubMed: 17166910]

Gilks N, Kedersha N, Ayodele M, Shen L, Stoecklin G, Dember LM, Anderson P. Stress granule assembly is mediated by prion-like aggregation of TIA-1. Mol Biol Cell 2004;15:5383–5398. [PubMed: 15371533]

Guil S, Long JC, Caceres JF. hnRNP A1 relocalization to the stress granules reflects a role in the stress response. Mol Cell Biol 2006;26:5744–5758. [PubMed: 16847328]

Ivanov PA, Chudinova EM, Nadezhdina ES. Disruption of microtubules inhibits cytoplasmic ribonucleoprotein stress granule formation. Exp Cell Res 2003;290:227–233. [PubMed: 14567982]

Kedersha N, Anderson P. Stress granules: sites of mRNA triage that regulate mRNA stability and translatability. Biochem Soc Trans 2002;30:963–969. [PubMed: 12440955]

Kedersha N, Chen S, Gilks N, Li W, Miller IJ, Stahl J, Anderson P. Evidence that ternary complex (eIF2-GTP-tRNA(i)(Met))-deficient preinitiation complexes are core constituents of mammalian stress granules. Mol Biol Cell 2002;13:195–210. [PubMed: 11809833]

Kiebler MA, Bassell GJ. Neuronal RNA granules: movers and makers. Neuron 2006;51:685–690. [PubMed: 16982415]

Kim SH, Dong WK, Weiler IJ, Greenough WT. Fragile X mental retardation protein shifts between polyribosomes and stress granules after neuronal injury by arsenite stress or in vivo hippocampal electrode insertion. J Neurosci 2006;26:2413–2418. [PubMed: 16510718]

Krichevsky AM, Kosik KS. Neuronal RNA granules: a link between RNA localization and stimulation-dependent translation. Neuron 2001;32:683–696. [PubMed: 11719208]

Lee KH, Lee S, Kim B, Chang S, Kim SW, Paick JS, Rhee K. Dazl can bind to dynein motor complex and may play a role in transport of specific mRNAs. Embo J 2006;25:4263–4270. [PubMed: 16946704]

Leung KM, van Horck FP, Lin AC, Allison R, Standart N, Holt CE. Asymmetrical beta-actin mRNA translation in growth cones mediates attractive turning to netrin-1. Nat Neurosci 2006;9:1247–1256. [PubMed: 16980963]

Ling SC, Fahrner PS, Greenough WT, Gelfand VI. Transport of Drosophila fragile X mental retardation protein-containing ribonucleoprotein granules by kinesin-1 and cytoplasmic dynein. Proc Natl Acad Sci U S A 2004;101:17428–17433. [PubMed: 15583137]

Lo KW, Kogoy JM, Rasoul BA, King SM, Pfister KK. Interaction of the DYNLT (TCTEX1/RP3) light chains and the intermediate chains reveals novel intersubunit regulation during assembly of the dynein complex. J Biol Chem 2007;282:36871–36878. [PubMed: 17965411]

Nonhoff U, Ralser M, Welzel F, Piccini I, Balzereit D, Yaspo ML, Lehrach H, Krobitsch S. Ataxin-2 interacts with the DEAD/H-box RNA helicase DDX6 and interferes with P-bodies and stress granules. Mol Biol Cell 2007;18:1385–1396. [PubMed: 17392519]

Ravikumar B, Acevedo-Arozena A, Imarisio S, Berger Z, Vacher C, O'Kane CJ, Brown SD, Rubinsztein DC. Dynein mutations impair autophagic clearance of aggregate-prone proteins. Nat Genet 2005;37:771–776. [PubMed: 15980862]

Stohr N, Lederer M, Reinke C, Meyer S, Hatzfeld M, Singer RH, Huttelmaier S. ZBP1 regulates mRNA stability during cellular stress. J Cell Biol 2006;175:527–534. [PubMed: 17101699]

Thomas MG, Martinez Tosar LJ, Loschi M, Pasquini JM, Correale J, Kindler S, Boccaccio GL. Staufen recruitment into stress granules does not affect early mRNA transport in oligodendrocytes. Mol Biol Cell 2005;16:405–420. [PubMed: 15525674]

Tsai NP, Bi J, Loh HH, Wei LN. Netrin-1 signaling regulates de novo protein synthesis of kappa opioid receptor by facilitating polysomal partition of its mRNA. J Neurosci 2006;26:9743–9749. [PubMed: 16988045]

Tsai NP, Bi J, Wei LN. The adaptor Grb7 links netrin-1 signaling to regulation of mRNA translation. Embo J 2007;26:1522–1531. [PubMed: 17318180]

Tsai NP, Ho PC, Wei LN. Regulation of stress granule dynamics by Grb7 and FAK signalling pathway. Embo J 2008;27:715–726. [PubMed: 18273060]

Umesono K, Murakami KK, Thompson CC, Evans RM. Direct repeats as selective response elements for the thyroid hormone, retinoic acid, and vitamin D3 receptors. Cell 1991;65:1255–1266. [PubMed: 1648450]

Vessey JP, Vaccani A, Xie Y, Dahm R, Karra D, Kiebler MA, Macchi P. Dendritic localization of the translational repressor Pumilio 2 and its contribution to dendritic stress granules. J Neurosci 2006;26:6496–6508. [PubMed: 16775137]

Wanschers B, van de Vorstenbosch R, Wijers M, Wieringa B, King SM, Fransen J. Rab6 family proteins interact with the dynein light chain protein DYNLRB1. Cell Motil Cytoskeleton 2008;65:183–196. [PubMed: 18044744]

Wu KY, Hengst U, Cox LJ, Macosko EZ, Jeromin A, Urquhart ER, Jaffrey SR. Local translation of RhoA regulates growth cone collapse. Nature 2005;436:1020–1024. [PubMed: 16107849]

Abbreviation

SG
: stress granule

DLC2A
: dynein light chain 2A

RNP complex
: ribonucleoprotein complex

TIA-1
: T cell internal antigen-1

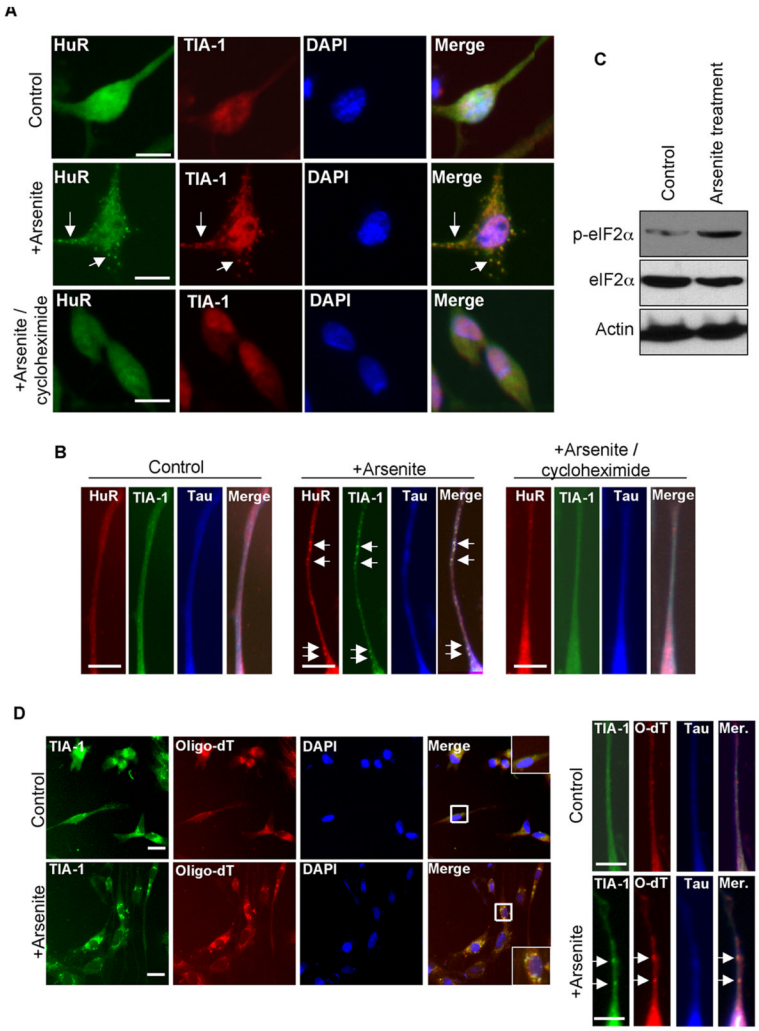

Figure 1. Arsenite induces stress granules in the soma and neurites of primary spinal cord neurons

(A) (B) Immunohistochemistry of control (A: top; B: left), arsenite-treated (A: middle; B: middle) or arsenite/cycloheximide-treated (A: bottom; B: right) neurons using anti-TIA-1 or anti-HuR antibodies. Clear punctates are marked by arrows. (C) The stress condition was examined on Western blots probed with anti-phospho-eIF2α, anti-eIF2α and anti-Actin antibodies. Actin was served for the lysate control. (D) Immunohistochemistry and fluorescence *in situ* hybridization of control (top left and top right) or arsenite-treated (bottom left and bottom right) spinal cord neurons with biotinylated Oligo(dT), followed by anti-TIA-1 detection. Merged images are shown on the right of each panel. Clear punctates are marked by arrows. Bars, 25 μm. Control, untreated; +Arsenite, 0.5 mM sodium arsenite treated.

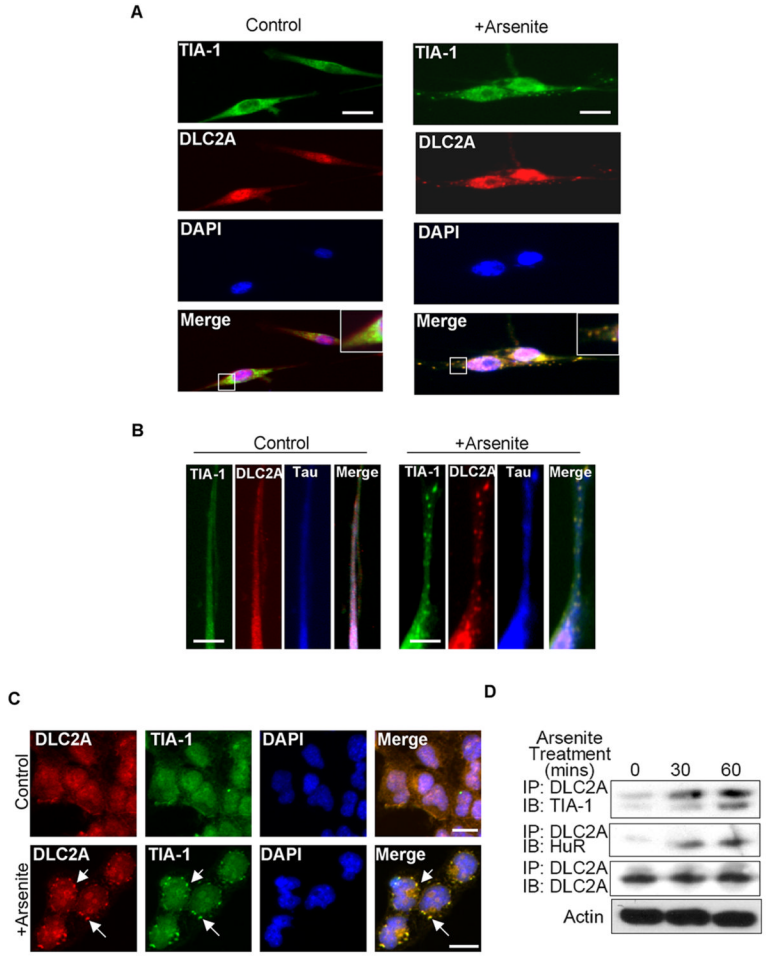

Figure 2. Dynein motor subunit DLC2A localizes in SGs

(A) Immunohistochemistry of control or arsenite-treated primary spinal cord neurons using antibodies against dynein light chain 2A (DLC2A) and TIA-1. Nucleus is stained by DAPI. Merged images are shown on the bottom. Enlarged boxed areas are shown on the top right. (B) Immunohistochemistry of arsenite-treated neurites of primary spinal cord neuron using antibodies against DLC2A, TIA-1 and Tau. Clear punctates are marked by arrows. (C) Immunohistochemistry of control- or arsenite-treated P19 cells using anti-TIA-1 and anti-DLC2A antibodies. Merged images are shown on the right. (D) Western blots of TIA-1 and HuR immunoprecipitated with anti-DLC2A from P19 cells treated with arsenite for 0, 30 or 60 minutes. Anti-DLC2A precipitates (IP control) and Actin (total lysate control) are shown on the two bottom panels. Bars, 25 μm. Control, untreated; +Arsenite, 0.5 mM sodium arsenite treated.

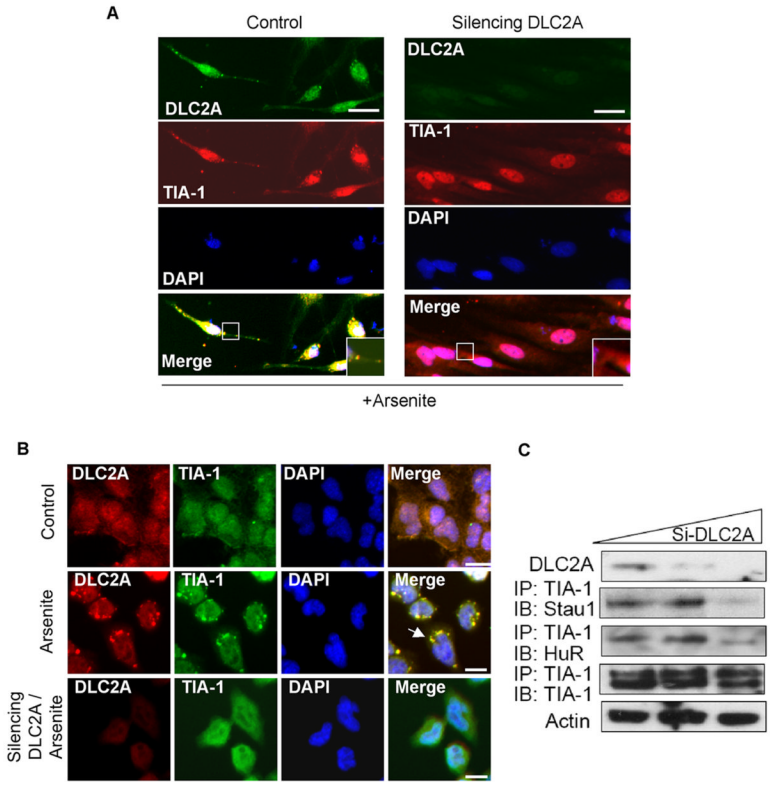

Figure 3. Dynein motor subunit DLC2A is required for SG formation

(A) Immunohistochemistry of arsenite-treated control (left) or DLC2A-silenced (right) primary spinal cord neurons using antibodies against TIA-1, together with DLC2A. All merged images are shown on the bottom. Enlarged boxed areas are shown on the bottom right. (B) Immunohistochemistry of control, arsenite-treated control (left) or DLC2A-silenced (right) (top to bottom)-treated P19 cells using anti-TIA-1 and anti-DLC2A antibodies. Bars, 25 μm. (C) Western blots of Staufen 1 (Stau) and HuR immunoprecipitated with anti-TIA-1 from arsenite-stressed P19 cells treated with increasing amounts of DLC2A siRNA. Anti-TIA-1 precipitates (IP control) and Actin control (total lysate control) are shown on the bottom two panels. The effects of silencing DLC2A were monitored as shown on the top. Control, untransfected; Silencing DCL2A, DLC2A siRNA transfected.

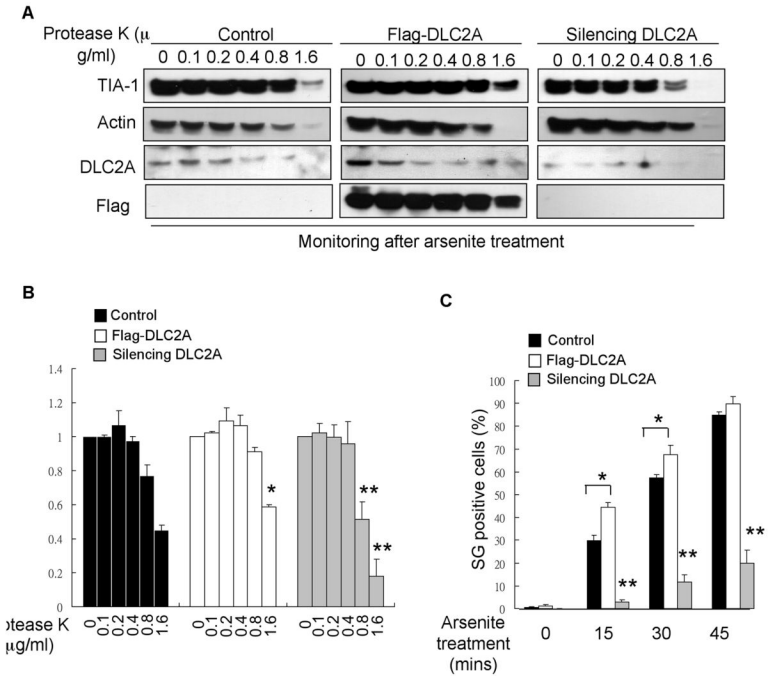

Figure 4. Dynein motor subunit DLC2A enhances SG integrity and formation rate

(A) Western blots of TIA-1, Actin, DLC2A and Flag from control, Flag-DLC2A transfected or DLC2A-silenced and arsenite-stressed P19 cytoplasmic protein treated with Protease K at 0, 0.1, 0.2, 0.4, 0.8 and 1.6 μg/ml respectively. (B) Quantification of TIA-1 intensities upon Protease K treatment from three independent experiments. ** represents significance between silencing DLC2A cells and control cells at the same time point, $P < 0.05$. * represents significance between Flag-DLC2A transfected cells and control cells at the same time point, $P < 0.05$. (C) Quantification of SG-positive cells transfected with control, Flag-DLC2A, or DLC2A siRNA after arsenite treatment for 0, 15, 30 or 45 minutes. Data are represented as mean +/- SEM. The significance between the control and Flag-DLC2A transfected cells was marked with * (*$P < 0.05$); the significance between silencing DLC2A and either the control or Flag-DLC2A transfected cells was marked with ** (**$P < 0.05$).

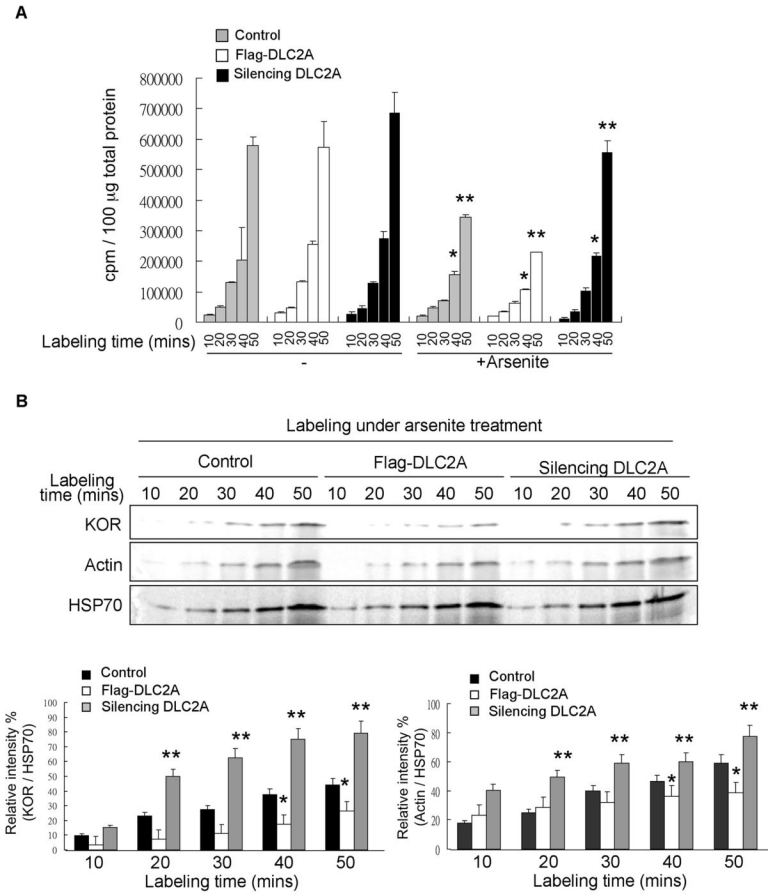

Figure 5. Dynein motor subunit DLC2A enhances translation repression

(A) Metabolic labeling to monitor total translation in control, Flag-DLC2A transfected or DLC2A siRNA-transfected P19 cultures in 10, 20, 30, 40 or 50 minutes ^{35}S-Methione/Cysteine incubation with (right) and without (left) arsenite treatment. *, ** represent significance between arsenite-treated control, Flag-DLC2A transfected or DLC2A siRNA-transfected cells at 40- or 50-minute time points respectively, $P < 0.05$. (B) Metabolic labeling to monitor KOR, Actin and HSP70 immunoprecipitated from control, Flag-DLC2A or DLC2A siRNA-transfected P19 cultures after 10, 20, 30, 40 and 50 minutes under arsenite treatment. Relative HSP70-normalized values were shown on the bottom. ** represents significance between silencing DLC2A cells and control cells, $P < 0.05$. * represents significance between Flag-DLC2A transfected cells and control cells, $P < 0.05$.

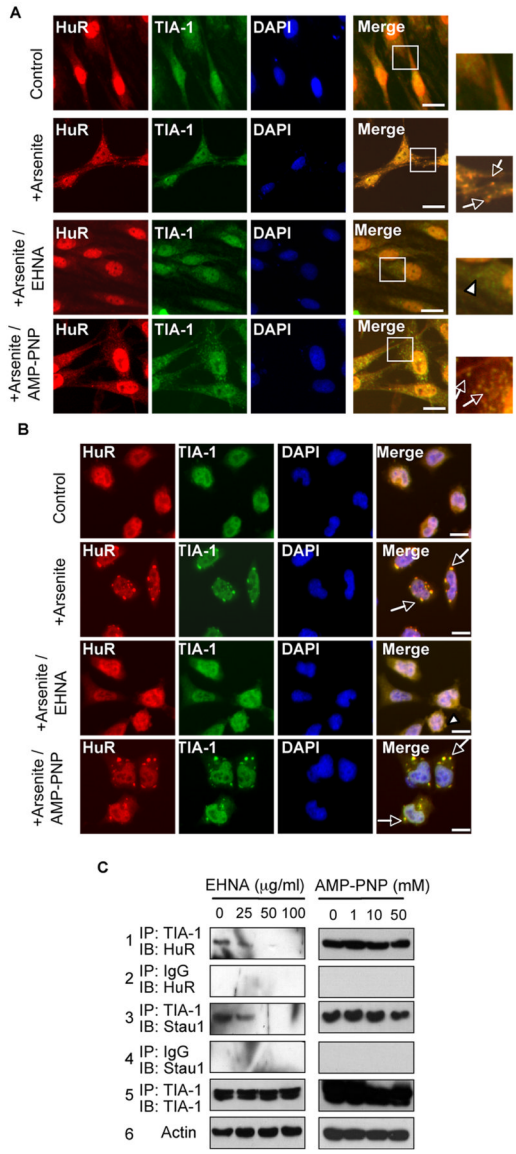

Figure 6. Dynein motor inhibitor attenuates SG formation

(A) (B) Immunohistochemistry of control-, arsenite, arsenite/EHNA- or arsenite/AMP-PNP treated primary spinal cord neurons (A) or P19 cells (B) using anti-TIA-1 and anti-HuR antibodies. Merged and/or enlarged areas are shown on the right. Clear punctates are marked by arrows. Some small granules in arsenite/EHNA-treated cells were marked by arrow heads. Bars, 25 μm. (C) Western blots of HuR and Staufen 1 (Stau 1) immunoprecipitated with anti-TIA-1 or IgG from arsenite-stressed P19 cells treated with increasing amounts of EHNA. TIA-1 precipitates (IP control) and Actin control (total lysate control) are shown on the bottom two panels.

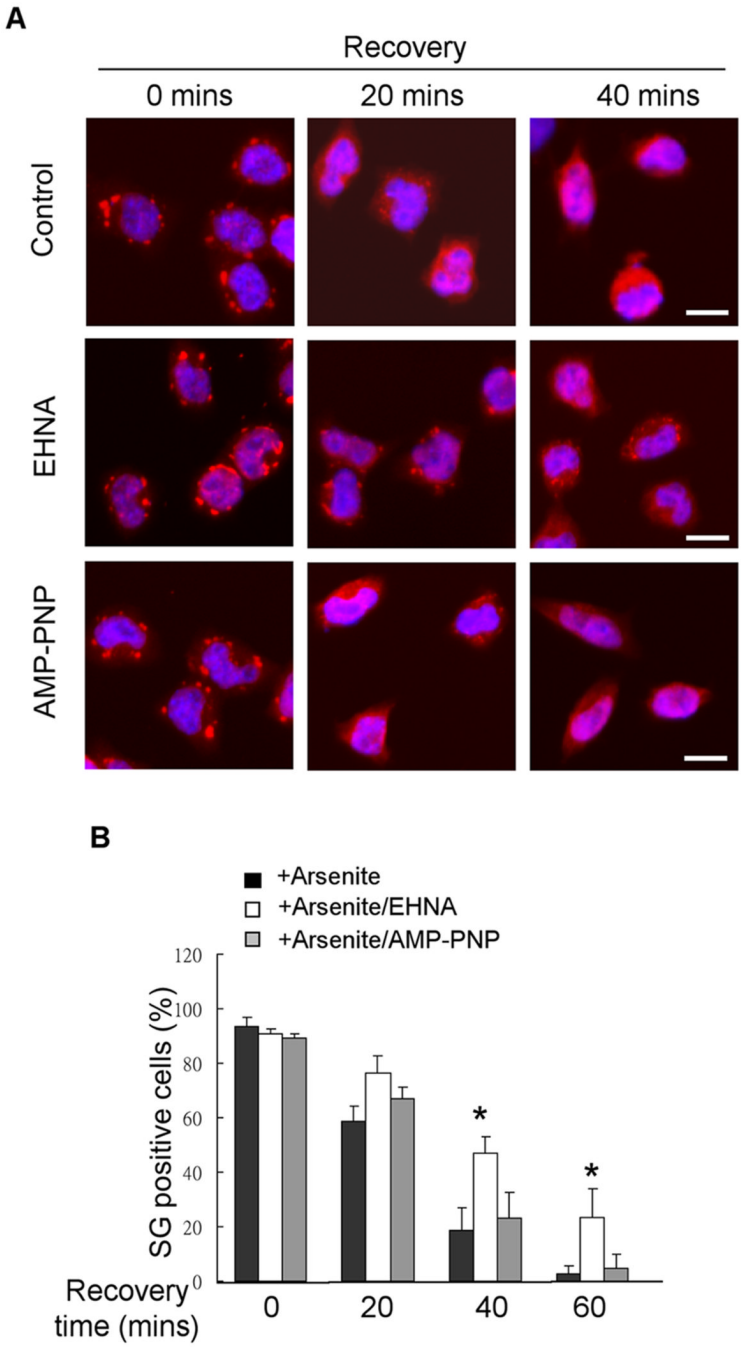

Figure 7. Dynein motor inhibitor attenuates SG disassembly

(A) Immunohistochemistry of control, EHNA (50 μg/ml) or AMP-PNP (1 mM) treated recovering P19 cells for 0, 20 or 40 minutes. Merged images of TIA-1 (red) and DAPI (blue) are shown. Bars, 25 μm. (B) Quantification by scoring SG-positive cells from (A) at 0-, 20-, 40- or 60- minute of recovery (*$P < 0.05$).